

Stiffener/Skin Interactions in Pressure-Loaded Composite Panels

M. W. Hyer*

Virginia Polytechnic Institute & State University, Blacksburg, Virginia

D. C. Loup†

David Taylor Research Center, Annapolis, Maryland
and

J. H. Starnes Jr.‡

NASA Langley Research Center, Hampton, Virginia

The deflection and strain responses of pressure-loaded graphite-epoxy panels clamped on all four edges and stiffened by "T"-type stiffeners are presented and discussed. Attention is focused on the strains and strain gradients in the stiffener and skin in the region of stiffener attachment. The effects of overall stiffener stiffness, flange thickness, and overall skin stiffness on the responses are discussed. Pressure levels up to 1 atm are considered. Results indicate that geometric nonlinearities are important at these pressure levels. Furthermore, overall stiffener stiffness has a significant effect on panel response, particularly the out-of-plane deformation, or pil- lowing, of the skin. Flange thickness, while not influencing overall panel response, has a strong influence on the strains in the attachment region. To a lesser extent, skin stiffness influences the strains in the attachment region. Results also indicate that the interface between the skin and the stiffener experiences two components of shear stress, in addition to a normal (peel) stress. This indicates that the skin/stiffener interface problem is three-dimensional in nature.

Introduction

THE separation of stiffeners from skins under static and fatigue loading conditions continues to be a serious problem in the design of composite structures. Because of the discontinuity of material and geometry at the skin/stiffener interface, the stresses in this area are quite severe and can lead to failure. The failure modes associated with these stresses and the need for improved analysis methods of predicting the failures has been noted by several investigators. Among the relatively recent, Knight and Starnes^{1,2} noted the skin/stiffener interface region as the point of failure initiation for flat and curved stiffened panels loaded in axial compression into the postbuckling range. Their finite-element analyses correlated well with their experimental results up to the point of failure initiation. A recent analytical investigation of the problem of skin/stiffener interactions in postbuckled panels, at a more detailed level, was given by Wang and Biggers.³ Dickson et. al.⁴ studied several methods of attaching stiffeners to panels in an effort to delay the onset of separation. These previous studies have contributed both to the development of analytical models and to the collection of data from actual experiments. The data that have been recorded, however, have usually dealt with the effects of the method of stiffener attachment, stiffener geometry, stiffener material properties, skin material properties, and other parameters on overall load capacity of stiffened panels. Little effort has been made to evaluate the effects of the parameters on strain distributions, de-

formations, or other indicators of the severity of the stress state near the skin/stiffener interface region. The present paper addresses that specific issue by discussing an experimental study that focused on the skin/stiffener attachment region of pressure-loaded graphite-epoxy panels. The effects of stiffener geometry and skin elastic properties on the strain distributions in the skin/stiffener attachment region are described. In particular, the effects of web heights, flange thicknesses, and skin stiffnesses on the strain distributions in pressure-loaded stiffened graphite-epoxy panels are examined. The effects of these parameters on the strain gradients in the region of the stiffener and skin interaction are also studied. Strain gradients in this region are felt to be as important as the strain magnitudes themselves and therefore were measured. The effects of a small amount of in-plane loading on panel response are also discussed.

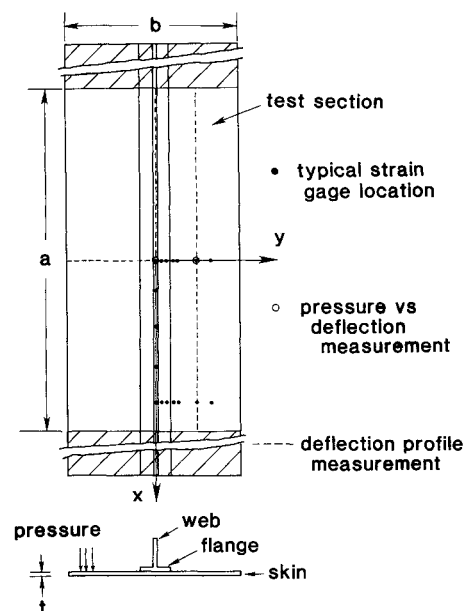


Fig. 1 Schematic of panels studied.

Presented in part as Paper 86-0917 at the AIAA/ASME/ASCE/AHS 27th Structures, Structural Dynamics, and Materials Conference, San Antonio, TX, May 19-21, 1986; received Oct. 6, 1986; revision received Oct. 14, 1988. Copyright © 1989 American Institute of Aeronautics and Astronautics, Inc. All rights reserved.

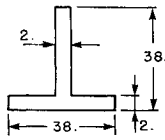
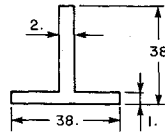
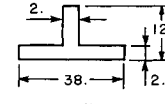
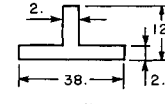
*Professor, Department of Engineering Science and Mechanics. Associate Fellow AIAA.

†Mechanical Engineer, Ship Materials Engineering Department. Member AIAA.

‡Head, Structural Mechanics Branch, Structures and Dynamics Division. Associate Fellow AIAA.

Table 1 Stiffener/skin combinations studied

Skin layup	[$\pm 45/0/90$] _s			[$\pm 45/90_2$] _s		
	Stiffness ratios:	In-plane	Bending	Stiffness ratios:	In-plane	Bending
Stiffener	longitudinal	1.0	1.28	longitudinal	0.47	0.95
Description, mm	transverse	1.0	1.0	transverse	1.53	1.33

	-Panel A	-Panel D
	-Quasi-isotropic skin	-Transversely stiff orthotropic skin
	-Tall stiffener web	-Tall stiffener web
	-Thick flange	-Thick flange
Web and flange layup [$\pm 45/0/90_2/0/\pm 45$] _s		
	-Panel B	(not studied)
	-Quasi-isotropic skin	
Web layup (same as above)	-Tall stiffener web	
	-Thin flange	
Flange layup [$\pm 45/0/90$] _s		
	-Panel C	(not studied)
	-Quasi-isotropic skin	
Web and flange layup [$\pm 45/0/90_2/0/\pm 45$] _s	-Short stiffener web	
	-Thick flange	

Description of Stiffened Panels

A schematic diagram of the panels studied is shown in Fig. 1. The x - y coordinate system used to describe the panels and their response is shown in the figure. In this paper, the direction parallel to the x axis will be referred to as the longitudinal direction and the direction parallel to the y axis will be referred to as the transverse direction. The panels consisted of a thin skin and a single discrete stiffener. The skins were eight layers, nominally 1 mm (0.040 in.) thick AS4/3502 graphite-epoxy. The panels were 1.22 m long by 0.56 m wide (48 × 22 in.). The test section of each panel was a central region 0.51 m long by 0.25 m wide (20 × 10 in.). The test section is indicated in Fig. 1. The reason for the panel being longer than the test section will be described shortly. Herein the length of the test section will be denoted by a , the width by b , and the thickness by t . The AS4/3502 "T" stiffener, which was secondarily bonded to the skin, was centered widthwise and spanned the entire length. While the width of the stiffener flange was maintained at 38 mm (1.5 in.) for all the panels tested, the web height and flange thickness were varied. The boundaries of the test section were clamped, and a maximum pressure level of just under atmospheric pressure (0.103 MPa, 14.7 psi (was used.)

The testing was limited to four different stiffened panel configurations. They will be referred to as panels A, B, C, and D. Three of the four panels had quasi-isotropic skins while the fourth panel had an orthotropic skin. The bending properties of both skins were such that no component of the bending stiffness matrix D_{ij} was zero. The stiffener on one of the four panels had a shorter web than the others, and the stiffener on other panel had a thinner flange. The geometric characteristics of the stiffener cross sections of the four panels are presented in Table 1, along with the ratios of both in-plane and bending stiffnesses of the skins relative to the transverse direction of the quasi-isotropic skin.

Panel A was considered to be the baseline panel. Panel B was identical to panel A in every respect except that the flange was thinner. Comparisons between panels A and B provided

information on the influence of flange thickness on the strains and strain gradients. Panel C was identical to panel A except for reduced web height. Comparisons between panels A and C provided direct information as to the influence of web height (effectively, the influence of both the location of the neutral axis and the stiffener cross section moment of inertia) on response near the stiffener attachment. Finally, panel D was identical to panel A except that the skin was orthotropic. The skin of panel D was softer longitudinally in in-plane stretching and in bending than the quasi-isotropic skin. However, in the transverse direction the orthotropic skin was stiffer both in in-plane stretching and in bending. This stiffness of the orthotropic skin was increased in the transverse direction to study the effect of the transverse bending stiffness of the skin on the degree of flange bending in the transverse direction.

Test Fixture

A photograph of the test fixture used to load the panels is shown in Fig. 2. Several of the primary features of the fixture are indicated in the figure. The backbone of the fixture was the vacuum plate, a 75-mm (3.0-in.)-thick steel plate with three recessed areas or cavities. The larger center cavity was 0.51 m long by 0.25 m wide (20 × 10 in.) and was used to load the test section of the composite panels by evacuating it with a vacuum pump. The smaller end cavities were also evacuated. Because of the dimensions of the composite panels, they covered the smaller end cavities and, in fact, extended beyond the vacuum plate. The stiffeners on the panels spanned all three cavities and also extended beyond the vacuum plate. Rubber O-rings provided a seal between the panel and the vacuum plate. With the cavities evacuated, the composite panel and the attached stiffener were pulled down over each of the three cavities. Three cavities were used in the stiffener direction so that the zero slope condition (a requirement for a clamped edge) on the stiffener at the end of the test section was guaranteed. Similar cavities could have been used in the other direction, i.e., making the vacuum plate with nine cavities. However, the cost and complexity of a larger vacuum

plate and the related test panels are deemed to be excessive for the scope of this study. It was also felt that the clamped condition for the longitudinal edges of the skin could be closely approximated by simple clamping.

The stretching frame used to preload the panels in biaxial tension is also shown in Fig. 2. The in-plane loads were transmitted from the frame to the panel by clevises. Steel doublers bonded around the circumference of the panel and steel pins through the doublers and the panel itself were used to transmit the load from the clevises to the test panel. Each clevis was connected to the stretching frame by a threaded rod. By tightening nuts on the rod, specific amount of tension could be applied to the panel. The clevises were instrumented with strain gages to form a load cell, the clevises being calibrated a priori relative to a calibrated load cell. A special clevis was used to apply an axial load to the stiffener. It was important to have the axial prestrain in the stiffener match the longitudinal prestrain in the skin.

After in-plane preloads were applied, the panels were clamped to the vacuum plate. Clamping was accomplished by bolting clamping bars to the top side of the panel, the bolts going through the clamping bars, the panels themselves, and the vacuum plate. The zero slope condition was being enforced on the ends of the panels by virtue of the two end cavities being evacuated. However, clamping was necessary along the longitudinal edges to enforce the zero slope condition there. In addition, fully clamped edges are restrained from any in-plane displacements, and so the clamping bars were also used on the skins at the end of the test section.

Electrical resistance strain gages were used to measure the strains on the top and bottom surfaces of the panels. Figure 1 illustrates typical positions of the strain gages. More will be said of specific gage positions later. Linear variable differential transformers were used to measure deflections and deformed panel profiles. Figure 1 also shows the positions where the deflection measurements were made. For each test, data were recorded throughout the application of pressure.

Test Results

To illustrate the overall character of panel responses and the differences among the panels, the out-of-plane deflection response of the four panels as a function of the applied pressure is shown in Fig. 3. The deflections w were measured at the geometric center of the panel, i.e., $x=0$, $y=0$ in Fig. 1, and at

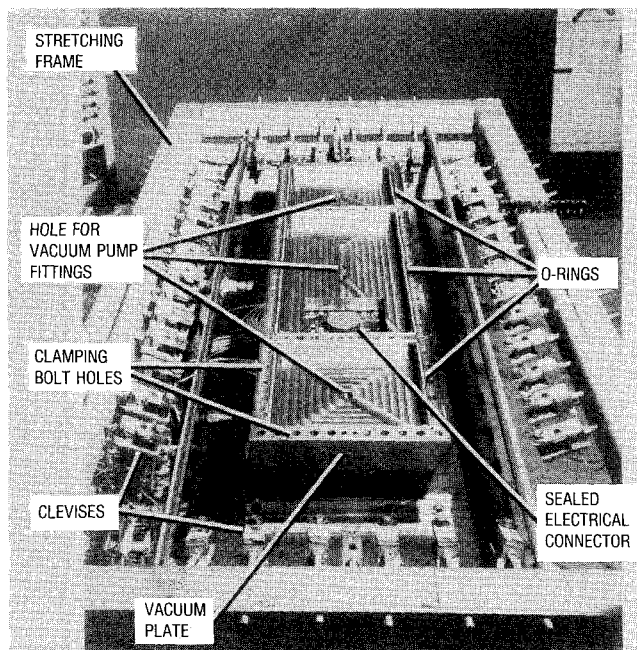


Fig. 2 Photograph of apparatus used to load panels.

midspan of the skin, halfway between the longitudinal centerline and the longitudinal edge, i.e., $x=0$, $y/b=0.25$. The response for the case of a light preload is illustrated in the figure. The solid lines show the deflections at the center of the panel while the dashed lines show the deflections of the skin. Several characteristics of the response are evident from the figure. First, the deflections were nonlinear functions of the applied pressure. The nonlinearity occurred at pressures as low as 0.1 atm. The nonlinearity was a direct result of the membrane effect. The degree of nonlinearity depended on the particular panel and the location on the panel. The center of panel C, the panel with a short-webbed stiffener, exhibited the greatest deflection and the strongest nonlinearity. The centers of panels A, B, and D, which all showed similar responses, deflected the least and exhibited the weakest nonlinearity. The skin deflection of panel D was the least of the skin deflections due to the skin of the panel being orthotropic. As stated earlier, the orthotropic skin was stiffer in the transverse direction than the quasi-isotropic skin. Since the transverse direction had the shorter span, the stiffness in that direction had an influence on deflections. The second interesting characteristic evident in the figure concerns the magnitude of the deflection of the skin relative to the deflection of the center. For panels A, B, and D, the deflection of the skin at $y/b=0.25$ was greater than the deflection of the center of the panel. For panel C, the deflection of the skin was less than the deflection of the center. The tall-webbed stiffeners on panels A, B, and D restrained the deflections at the centers of those panels while the short-webbed stiffener of panel C provided much less restraint at the center. The phenomenon of the skin deflecting more than the stiffener is referred to as *pillowing*; more will be said of this later.

Also shown in Fig. 3 is the result of a STAGS finite-element analysis.⁵ The intent of the analysis was to determine if the basic nonlinear characteristics of the response could be modeled with a general-purpose code. From Fig. 3 it can be concluded that this is indeed the case. A better correlation between numerical and experimental results could be realized if boundary flexibility was part of the finite-element analysis. That was beyond the scope of the present study.

The effect of the out-of-plane deflections of applying a biaxial in-plane load is seen in Fig. 4. Due to an increased membrane effect, all deflections were reduced relative to the no-preload case. This was particularly true of the skin deflections. However, the basic characteristics of the light preload case were retained.

As indicated in Figs. 3 and 4, the deflections encountered were several times the skin thickness. At the centers of the stiffener panels, the deflections were about two times the skin thick-

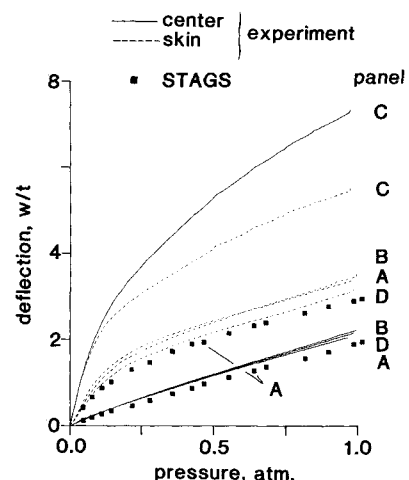


Fig. 3 Pressure-deflection characteristics of panels, light in-plane preload.

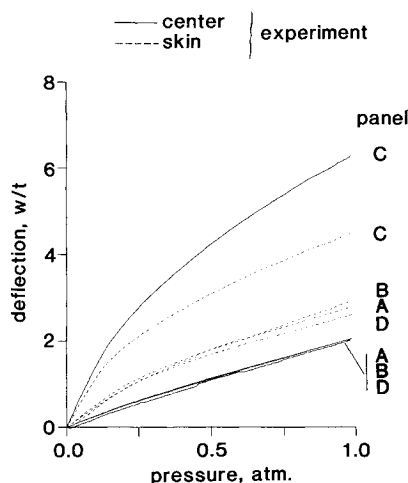


Fig. 4 Pressure-deflection characteristics of panels, biaxial in-plane preload.

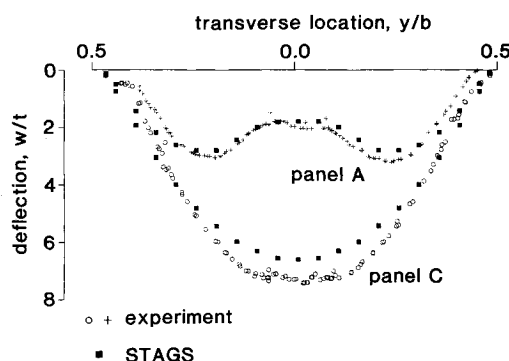


Fig. 5 Transverse profiles of the out-of-plane deflections of panels A and C at maximum pressure.

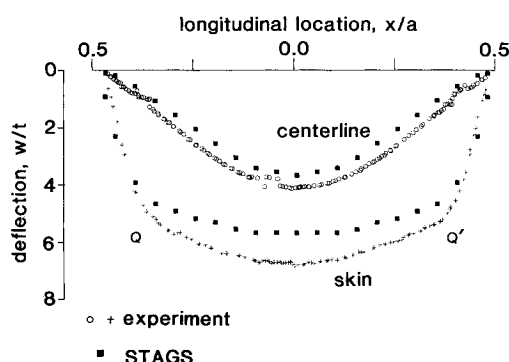


Fig. 6 Longitudinal profiles of the out-of-plane deflections of skin and centerline for panel A at maximum pressure.

ness. Away from the center, the deflections were about three times the skin thickness. For the softer panel, panel C, deflections up to seven skin thicknesses were encountered. Though deflections can be high, the main concern with stiffened composite panels is not so much with the magnitude of the deflection as it is with the fact that the skin relative to the stiffener that causes the high normal (peel) stresses at the skin/stiffener interface region. With stiffeners on the inside of a fuselage, internal fuselage pressure will cause this deflection of the skin relative to the stiffener and the accompanying severe stresses in the interface region. This pillowing effect is better demonstrated in the next figure.

Transverse deflection profiles for two of the panels are shown in Fig. 5. The figure shows the out-of-plane deflections

for panels A and C as a function of transverse distance from the centerline. The deflections are for the case of maximum pressure and the profile is along $x=0$. Figure 1 shows the location of this transverse profile. Comparisons of the transverse profiles of the two panels illustrate the pillowing effect evident in the panels with the tall-webbed stiffeners, the skin deflecting out-of-plane more than the skin/stiffener combination. It is clear that the dominance of the stiffener near the center of the panel was responsible for the effect. Though the details cannot be seen in this figure, with pillowing there was significant bending of both the stiffener flange and the skin near the flange. Because of the thinness of the skin, the skin experienced much larger bending strains than the flange. Also, compared to the skin strains away from the flange, i.e., at $x=0$, $y/b=0.25$, the skin strains near the flange were high. The transition from low to high values occurred in a narrow region near the flange. As will be seen, this effect led to high strain gradients near the flange.

Gradients were also observed that were associated with the longitudinal deflection profiles. Figure 6 shows two longitudinal deflection profiles for panel A, a centerline profile and a skin profile. The figure shows the out-of-plane deflections as a function of longitudinal position x . The centerline profile was measured along the line $y=0$ while the skin profile was measured along the line $y/b=0.25$. As shown in Fig. 1, the former profile measures the deflection response of the skin/stiffener combination at the centerline while the latter profile measures the deflection of the skin away from the stiffener. The pillowing of the skin is evident in this figure. However, another feature is also evident. This is as follows: the deflection profile of the skin has a more or less constant curvature over the span Q to Q' and then develops rather sharp curvatures near points Q and Q' . On the other hand, the deflection profile of the skin/stiffener combination does not have sharp curvatures at Q and Q' . Consequently, as the transition from $y/b=0.25$ to $y/b=0$ is made, the sharp curvatures in the skin at locations Q and Q' must be flattened to be compatible with the stiffener. This produces more severe interactions between the skin and stiffener than at points where the two curvatures are more compatible.

Deflection profiles from the STAGS analysis are also illustrated in Figs. 5 and 6. It is again clear that the correlation between the experimental and numerical results is good, including the sharp transition in skin curvature at locations Q and Q' .

The effects of pillowing and the dominance of the stiffener can be further illustrated by examining the strain distributions. Figure 7 shows the transverse bending strains as a function of transverse location in the flange/skin combination and in the skin near the flange for the four panels studied. Each portion of the figure illustrates the geometry of each of the panels in the flange region and indicates the location of the back-to-back strain gages. Even though the gages were small, relative to the scale of the geometry of the region, the strain values should be interpreted as average values under the gage. Figure 7 indicates the values of strain recorded at the panel midspan ($x=0$) for both the light and biaxial preload cases. The data shown were recorded at the maximum applied pressure.

The light preload case (circles and solid line) in Fig. 7 illustrates the large jump or increase in bending strain that occurred in the transition from the flange/skin combination to just the skin. Of the three panels with the tall stiffener webs, panel A appeared to experience the largest skin bending strains. In addition, the change of strain from the flange to the skin for panel A was the most severe change experienced for these three stiffer panels. Of these three panels, panel B with the thinner flange experienced the smallest bending strains in the skin. The orthotropic skin, panel D, has smaller bending strains relative to panel A, but they were somewhat larger than those for panel B. The skin bending strains were highest for the gage closest to the flange, and the other skin gage showed

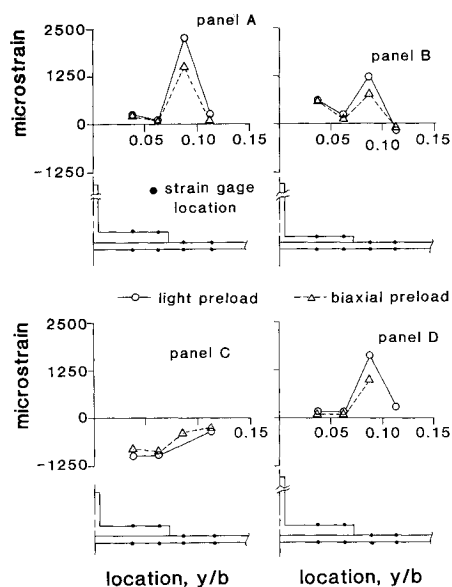


Fig. 7 Transverse bending strains vs transverse location in the stiffener interaction region at midspan ($x/a = 0$).

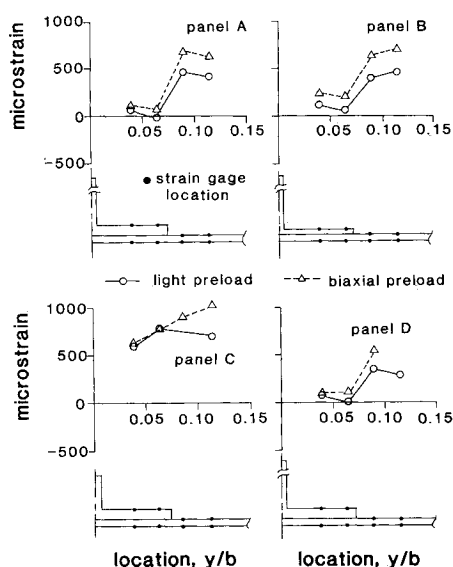


Fig. 8 Transverse membrane strains vs transverse location in the stiffener interaction region at midspan ($x/a = 0$).

lower strains. This difference indicates how localized the high strain levels were.

In contrast to panels A, B, and D, the softness of the stiffener of panel C was reflected in the sign of the bending strains for that panel. The skin of panel C was close to being in a state of pure membrane strain, and it was the stiffener flange that experienced the large bending strains. The large bending strains in the flange of panel C, rather than in the skin, were the opposite of the strain distribution in the other three panels. Since Figs. 3 and 4 indicate that the overall deflection behavior of panels A, B, and D were similar, the data of Fig. 7 indicate that panel A was the least desirable configuration of the three when considering local strain behavior.

Application of biaxial in-plane preload (triangles and dashed line) reduced the transverse bending strains at the maximum pressure level. This reduction was apparently due to the membrane stiffening effect that reduced the deflection levels, and thus the strain levels, relative to the light preload case.

The characteristics of the transverse membrane strains as a function of transverse location in the flange/skin region for

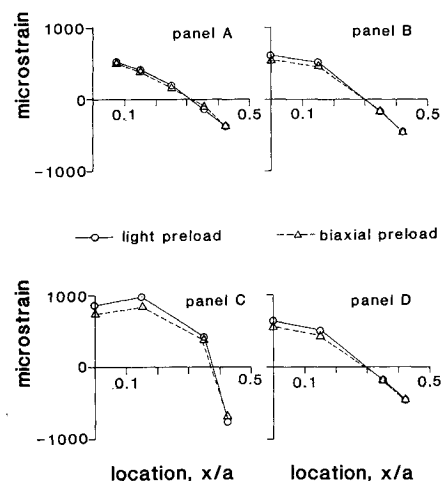


Fig. 9 Longitudinal strains vs longitudinal location on centerline below stiffener.

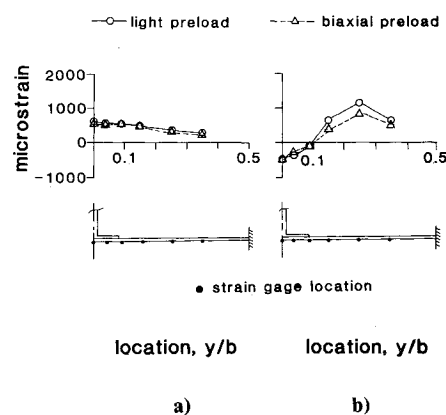


Fig. 10 Longitudinal strains vs transverse location, panel B: a) at $x/a = 0$; b) at $x/a = 0.425$.

the four panels are shown in Fig. 8. The strain data are for the case of maximum applied pressure. As can be seen and expected, the application of in-plane preload resulted in higher membrane strain levels. The flange strains were much less than the skin strains for all panels except panel C. The large center deflections of panel C (see Figs. 3 and 4) caused the membrane strain effects to be the greatest in panel C. However, the transverse membrane strains in the flange were larger, relative to the skin, than expected. The transversely stiffer skin of panel D somewhat reduced the transverse membrane strains.

While Figs. 7 and 8 illustrate one detail of the spatial variation of strains, a second detail can be illustrated by examining the variation of strain in the longitudinal direction. This detail is important because it indicates that the skin/stiffener interface stress problem is in fact a three-dimensional one. The variation of the longitudinal strain in the skins as a function of longitudinal location along the panel centerline directly below the stiffener web is illustrated in Fig. 9. This longitudinal strain is the total strain, not the bending or membrane component. Though not all panels had strain gages at the same locations along the centerline, the character of the spatial variation for each panel is evident. Specifically, the skin of each panel was in tension in the longitudinal direction at midspan ($x = 0$). Moving from midspan toward the end of the panel, the tensile strain decreased and the skin eventually experienced a compressive strain. The stiffener acted as a clamped/clamped beam and the flange, being below the neutral axis of the stiffener, experienced tensile strains near midspan and compressive strains near its clamped ends. The skin, being attached

to the flange, was forced to follow the strain response of the flange. Though seemingly a negligible effect, the implications of this behavior are far-reaching.

First, a significant longitudinal component of shear stress must act at the interface between the skin and the flange in order to force the skin to follow the flange. Specifically, a shear stress component τ_{xz} must exist. This shear stress is in addition to the peel-type tensile stress σ_z that is generated due to pillowing. The transverse gradients of strain, discussed earlier in connection with Fig. 7, imply that a component of shear stress τ_{yz} also acts at the interface. Therefore, all three components of stress exist at the interface. However, the stress problem could still be solved with a planar analysis (stresses depending only on y and z) if it were not for the fact that the shear stress τ_{yz} required to force the skin to follow the flange must vary within x or the longitudinal strain would not vary with x . As shown in Fig. 9, the strain does indeed change with x . This makes the skin/stiffener interface problem truly three-dimensional. Attempts have been made to study stiffener/skin separation experimentally by supporting the four edges of the panel and simply pulling on the stiffener in a direction normal to the panel. Based on the data presented herein on the gradients of longitudinal strain, it appears that this approach is an oversimplification of the problem for pressure-loaded panels.

The data of Fig. 9 do not show any significant differences in longitudinal strains among the three stiffer panels. Panel C, with its greater deflections, exhibits the largest strains. Also, the longitudinal strains of panel C, with its more flexible stiffener, changed from tension to compression much nearer to the clamped end of the stiffener than they did for the three panels with stiff stiffeners.

A final illustration of the strain levels and the strain gradients near the flange/skin interface is shown in Fig. 10. The longitudinal skin strains at the midspan and near the end of a panel with a tall webbed stiffener, specifically panel B, are shown in this figure as a function of transverse location. The gages were on the bottom surface of the skin. The longitudinal strain vs transverse location at the midspan location ($x=0$) is shown in Fig. 10a. The strains were tensile for all transverse locations, the strain levels decreasing monotonically from the panel centerline to the panel edge. These data serve as a basis for comparison with the data of Fig. 10b. This figure shows the longitudinal strain vs transverse location near the clamped end of the panel ($x/a=0.425$). These strain data varied from compression at the centerline to tension away from the centerline. As stated earlier, the flange forced the skin into compression at the centerline near the end of the panel. However, away from the centerline, the out-of-plane deflections coupled with the membrane effect and forced the skin into tension. Thus, there was a gradient of these longitudinal strains in the y direction, and the change from compression near the centerline to tension away from the centerline was the result of the flange/skin interactions. Comparing Figs. 10a and 10b illustrates the longitudinal gradient shown in Fig. 9, where centerline skin strains are tensile at midspan and compressive near the clamped end. With the format of Fig. 10, the strain gradients in both the longitudinal and transverse directions are illustrated.

It should be noted that no attempts were made to correlate numerical strain calculations with experimental measure-

ments. A more refined model of the flange/skin region than was afforded by the structural-level STAGS analysis would be necessary to obtain a realistic correlation. It should also be noted that no failures occurred during any of the testing. It is not clear what pressure levels will cause failure. That is an area of future work.

Conclusions

The most important conclusion of the study is that the interaction between the stiffener and the skin is a three-dimensional problem, not simply one-dimensional or two-dimensional as is often assumed. There are strain gradients in both directions, indicating skin/stiffener interactions in both the transverse and longitudinal directions. The results of the study indicate that two components of shear stress and a normal stress must exist at the interface between the skin and the stiffener flange. The normal stress is generated due to the out-of-plane deflection or pillowing, and the shear stresses are generated due to bending in the two directions. The results of this study indicate that the stiffness of the stiffener controls the degree of pillowing. In addition, the study shows that the panel with a thick stiffener flange experienced the largest transverse strain in the skin and the largest transverse bending strain gradient. The panel with a thin stiffener flange experienced the least amount of transverse bending strain. The longitudinal strains for these three cases were similar. For the panel with the short-webbed stiffener, the flange experienced larger transverse bending strains than the skin. Finally, it was found that geometric nonlinearities were important for the panels studied. This was true even for relatively low pressures. In closing, it is felt that the findings of this experimental effort will help direct other researchers in their studies of this complex and important problem.

Acknowledgments

The work reported herein was supported by the NASA-Virginia Tech Composites Program Cooperative Agreement NAG 1-343 between the NASA Langley Research Center and Virginia Polytechnic Institute and State University. The second author was formerly associated with the University.

References

- ¹Starnes, J. H., Jr. and Knight, N. F., Jr., "Postbuckling Behavior of Selected Flat Stiffened Graphite-Epoxy Panels Loaded in Compression," *Proceedings of the 23rd AIAA/ASME/ASCE/AHS Structures, Structural Dynamics, and Materials Conference*, AIAA, New York, 1982.
- ²Knight, N. F., Jr. and Starnes, J. H., Jr., "Postbuckling Behavior of Selected Curved Stiffened Graphite-Epoxy Panels Loaded in Compression," *Proceedings of the 26th AIAA/ASME/ASCE/AHS Structures, Structural Dynamics, and Materials Conference*, AIAA, New York, 1985.
- ³Wang, J. T. S. and Biggers, S. B., "Skin/Stiffener Interface Stresses in Composite Stiffened Panels," NASA CR-172261, Jan. 1984.
- ⁴Dickson, N. J., Biggers, S. B., and Starnes, J. H., "Stiffener Attachment Concepts for Graphite-Epoxy Panels Designed for Postbuckling Strength," presented at the 7th DOD/NASA Conference on Fibrous Composites in Structural Design, Denver, CO, June 1985.
- ⁵Almroth, B. O. and Brogan, F. A., "The STAGS Computer Code," NASA CR-2950, Feb. 1978.